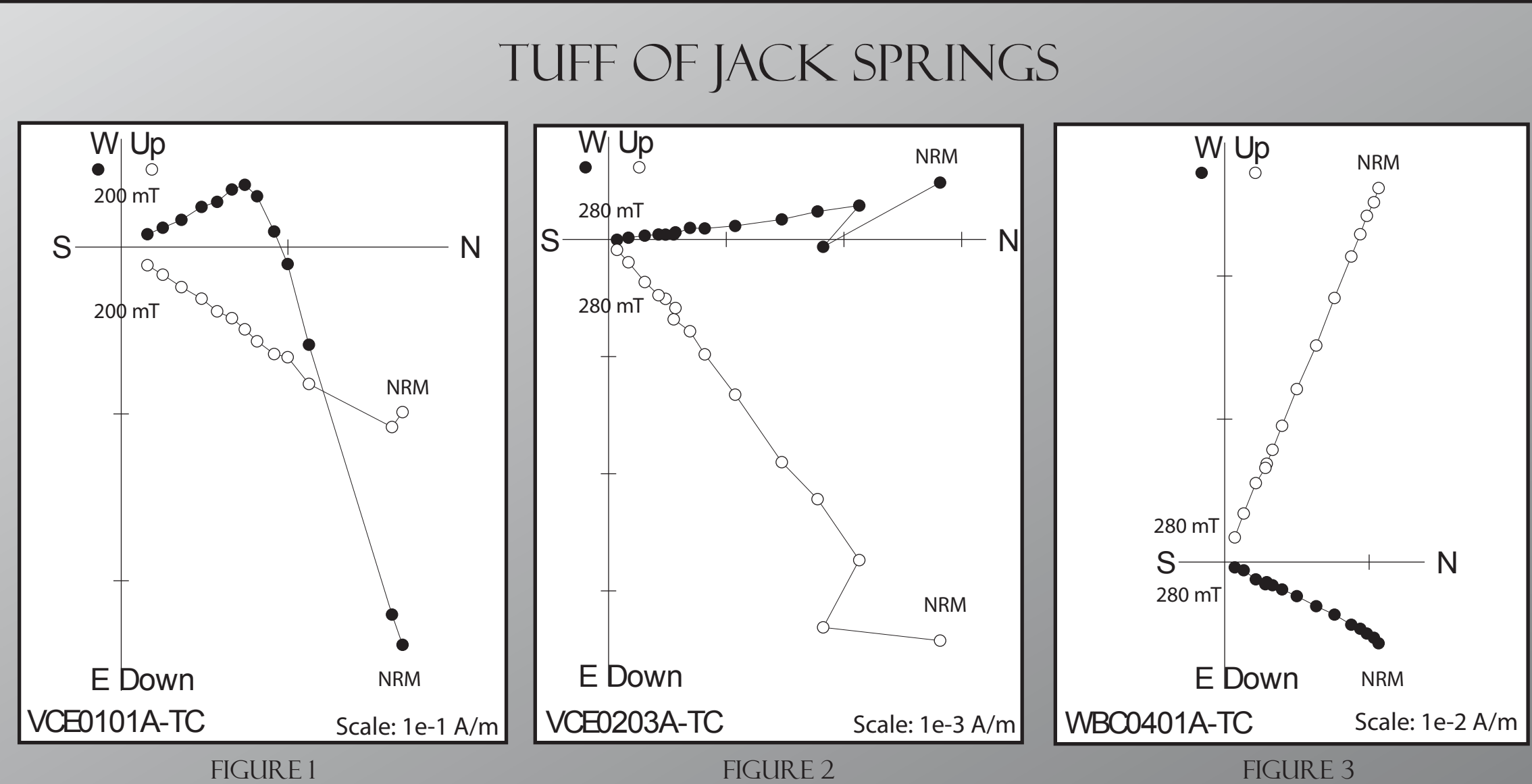
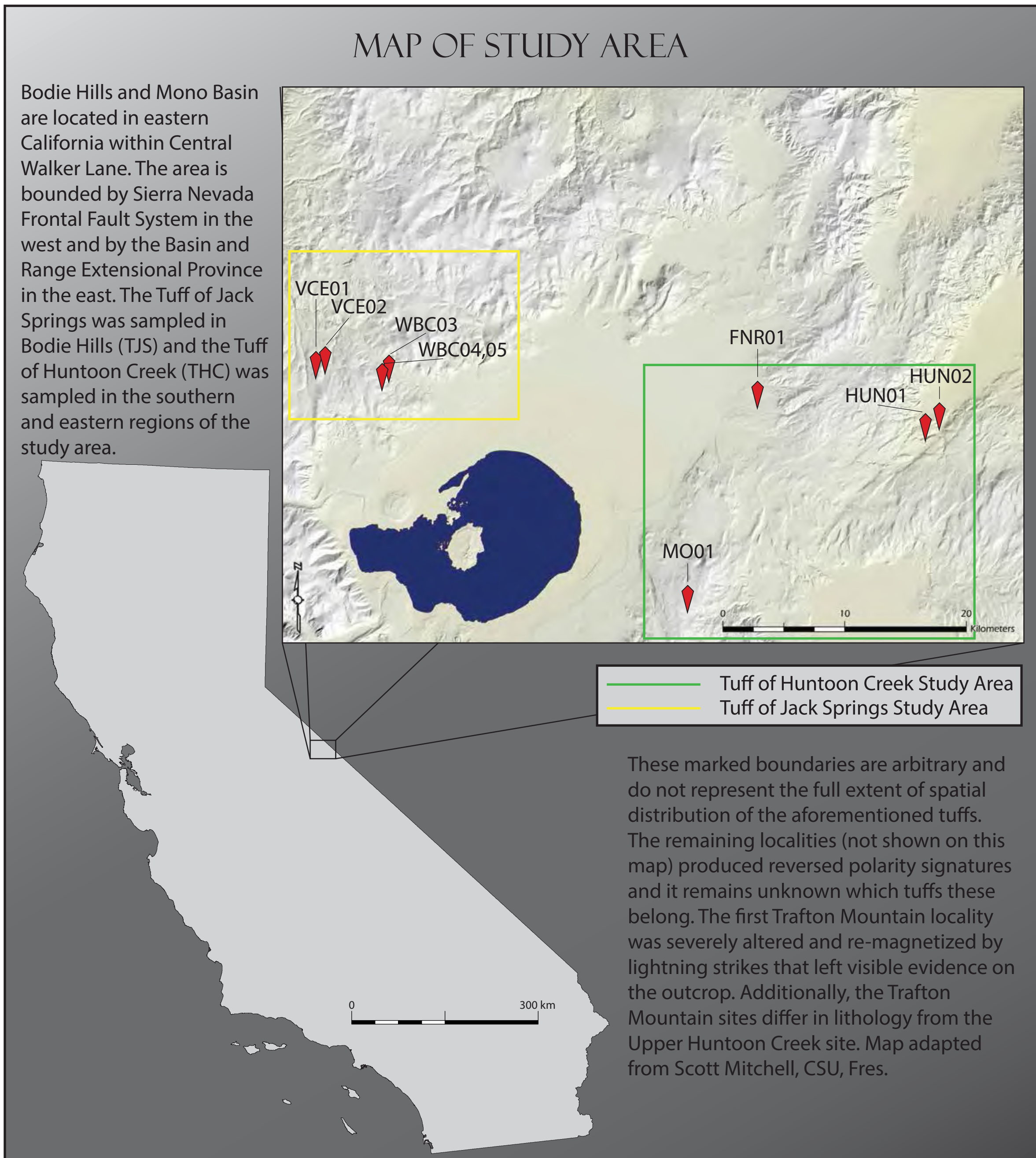


# POST-MIDDLE MIOCENE TUFFS OF BODIE HILLS AND MONO BASIN, CALIFORNIA: PALEOMAGNETIC REFERENCE DIRECTIONS AND VERTICAL AXIS ROTATION

LINDEMAN, JUSTIN R.; FLUHAR, CHRISTOPHER J.; FARNER, MICHAEL<sup>2</sup>  
<sup>1</sup>DEPARTMENT OF EARTH AND ENVIRONMENTAL SCIENCES, CALIFORNIA STATE UNIVERSITY, FRESNO, FRESNO, CA  
<sup>2</sup>DEPARTMENT OF EARTH SCIENCES, RICE UNIVERSITY, HOUSTON, TX  
JLINDEMAN@MAIL.FRESNOSTATE.EDU

FRESNO STATE  
Discovery. Diversity. Distinction.

The relative motions of the Pacific and North American plates about the Sierra Nevada-North American Euler pole is accommodated by dextral slip along the San Andreas Fault System (~75%) and the Walker Lane-Eastern California Shear Zone system of faults, east of the Sierra Nevada microplate (~25%). The Bodie Hills and Mono Basin regions lie within the Walker Lane and partially accommodate deformation by vertical axis rotation of up to 60° rotation since ~9.4 Ma. This region experienced recurrent eruptive Events from mid to late Miocene, including John et al.'s (2012) ~12.05 Ma Tuff of Jack Springs (TJS) and Gilbert's (1968) 11.1 – 11.9 Ma "latite ignimbrite" east of Mono Lake. Both tuffs can be identified by phenocrysts of sanidine and biotite in hand specimens, with TJS composed of a light-grey matrix and the latite ignimbrite composed of a grey-black matrix. Our paleomagnetic results show these units to both be normal polarity, with the latite ignimbrite exhibiting a shallow inclination. TJS's normal polarity is consistent with emplacement during subchron C5 An. 1n (12.014 – 12.116 Ma). The X-ray fluorescence analyses of fiamme from TJS in Bodie Hills and the latite ignimbrite located east of Mono Lake reveal them both to be rhyolites with the latite ignimbrite sharing elevated K composition seen in the slightly younger Stanislaus Group (9.0 – 10.2 Ma). We establish a paleomagnetic reference direction of  $D = 357.8^\circ I = 39.6^\circ \alpha_{95} = 4.4^\circ n = 5$  sites (42 samples) for TJS in the Bodie Hills in a region hypothesized by Carlson (2012) to have experienced low rotation. Our reference for Gilbert's latite ignimbrite (at Cowtrack Mountain) is  $D = 352.9^\circ I = 32.1^\circ \alpha_{95} = 4.7^\circ$ . This reference locality is found on basement highland likely to have experienced less deformation than the nearby Mono Basin since ignimbrite emplacement. Paleomagnetic results from this latite ignimbrite suggests  $\sim 94.5^\circ \pm 6.5^\circ$  of clockwise vertical axis rotation of parts of eastern Mono Basin since unit emplacement. A welded 11.7 Ma (K-Ar; Drake, 1979) rhyolitic tuff near Trafton Mountain appears similar in composition to TJS. Drake's tuff exhibits a reversed polarity, consistent with reversed polarity subchron C5r.3r (11.614 – 12.014 Ma) and distinguishes this tuff from TJS and Gilbert's latite ignimbrite.



Figures 1-3: Typical zijdelds from TJS sites showed overprints likely from lightning strikes. Alternating field demagnetization typically removed the signatures at 15–20 mT. All VCE01 samples demagnetized at steps 0, 2, 5, 10, 15, 20, 30, 45, 60, 80, 100, 130, 160, and 200 mT at CSU, Fresno Paleomagnetism Laboratory using a shielded single-axis 2G AF Demagnetizer. VCE02 and all WBC03, 04, 05 specimens were demagnetized at steps, 5, 10, 15, 20, 30, 40, 50, 60, 70, and 80 mT at the Paleomagnetism Laboratory at USGS, Menlo Park using a multi-specimen fully automated cryogenic magnetometer and additional steps 100, 140, 200, and 280 mT were completed at CSU, Fresno Paleomagnetism Laboratory. All CSU, Fresno magnetic field measurements taken in an AGICO JR6 magnetometer.

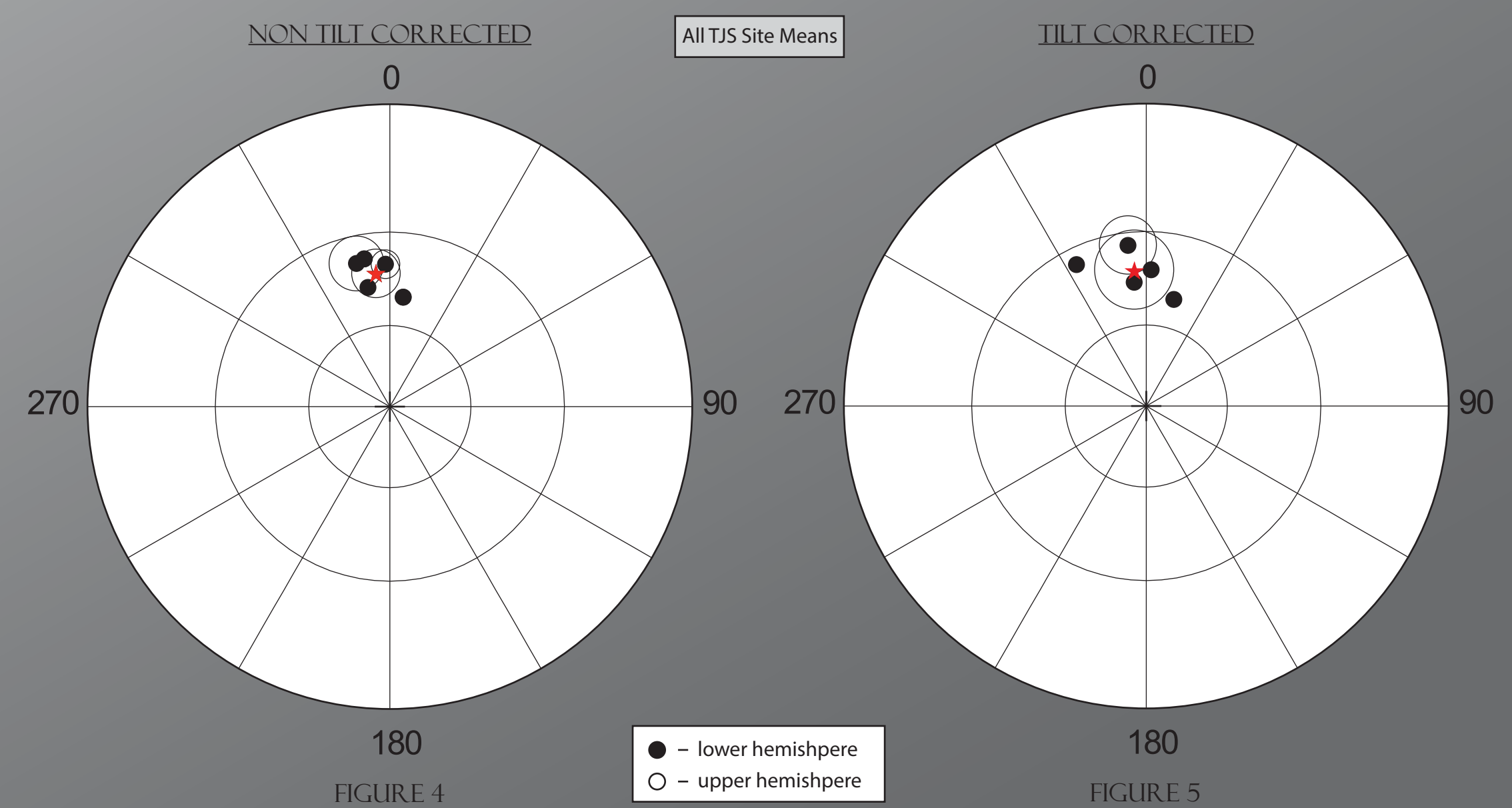


Figure 4: Characteristic remanent magnetizations (ChRM) of VCE01, VCE02, WBC03, WBC04, and WBC05 without tilt corrections. Red star indicates Fisher mean. For fig. 3 & 4,  $D = 353.5^\circ$ ,  $I = 42.5^\circ$ ,  $\alpha_{95} = 7.7^\circ$ ,  $D = 354.7^\circ$ , and  $I = 41.8^\circ$ . Figure 6: VCE01 outcrop. TJS can be identified in hand specimen by phenocrysts of sanidine and biotite. TJS has eutaxitic texture from which orientations were obtained. Chris for scale.

Result	SiO <sub>2</sub>	TiO <sub>2</sub>	Al <sub>2</sub> O <sub>3</sub>	Fe <sub>2</sub> O <sub>3</sub>	MnO	MgO	CaO	Na <sub>2</sub> O	K <sub>2</sub> O	P <sub>2</sub> O <sub>5</sub>	Cr <sub>2</sub> O <sub>3</sub>
WBC03	73.23	0.43	14.94	1.29	0.04	0.71	0.89	2.80	5.41	0.04	0.02
MO01	71.77	0.34	14.39	1.68	0.08	0.29	1.15	3.94	4.90	0.063	0.001
MO02	70.38	0.38	15.61	2.49	0.08	0.59	1.80	4.08	5.07	0.125	0.001
MO08	71.3	0.27	14.24	1.46	0.07	0.23	0.97	3.76	5.70	0.076	0.001
MO11	72.74	0.26	14.71	1.45	0.07	0.24	1.00	3.87	5.59	0.048	0.002

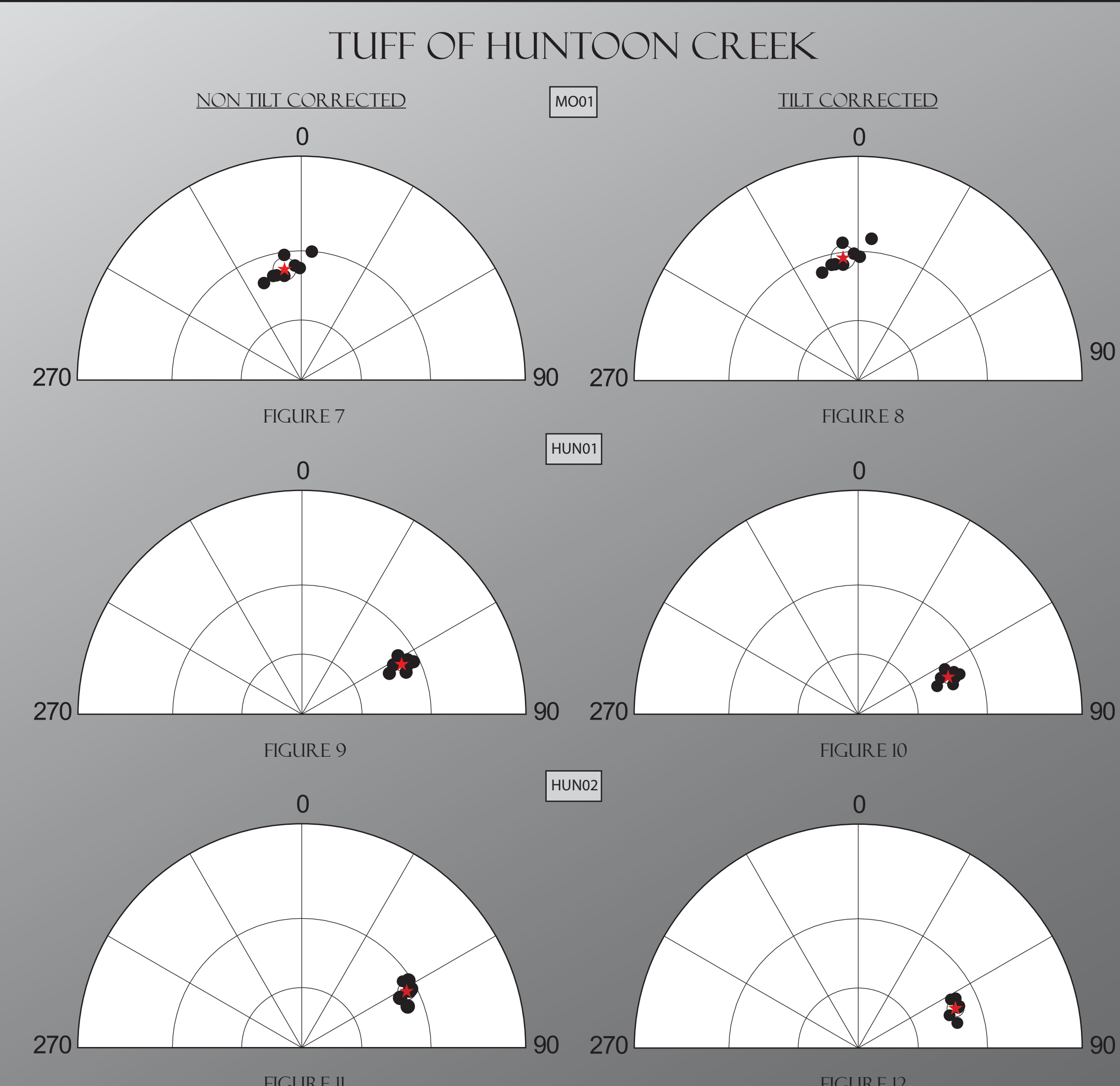
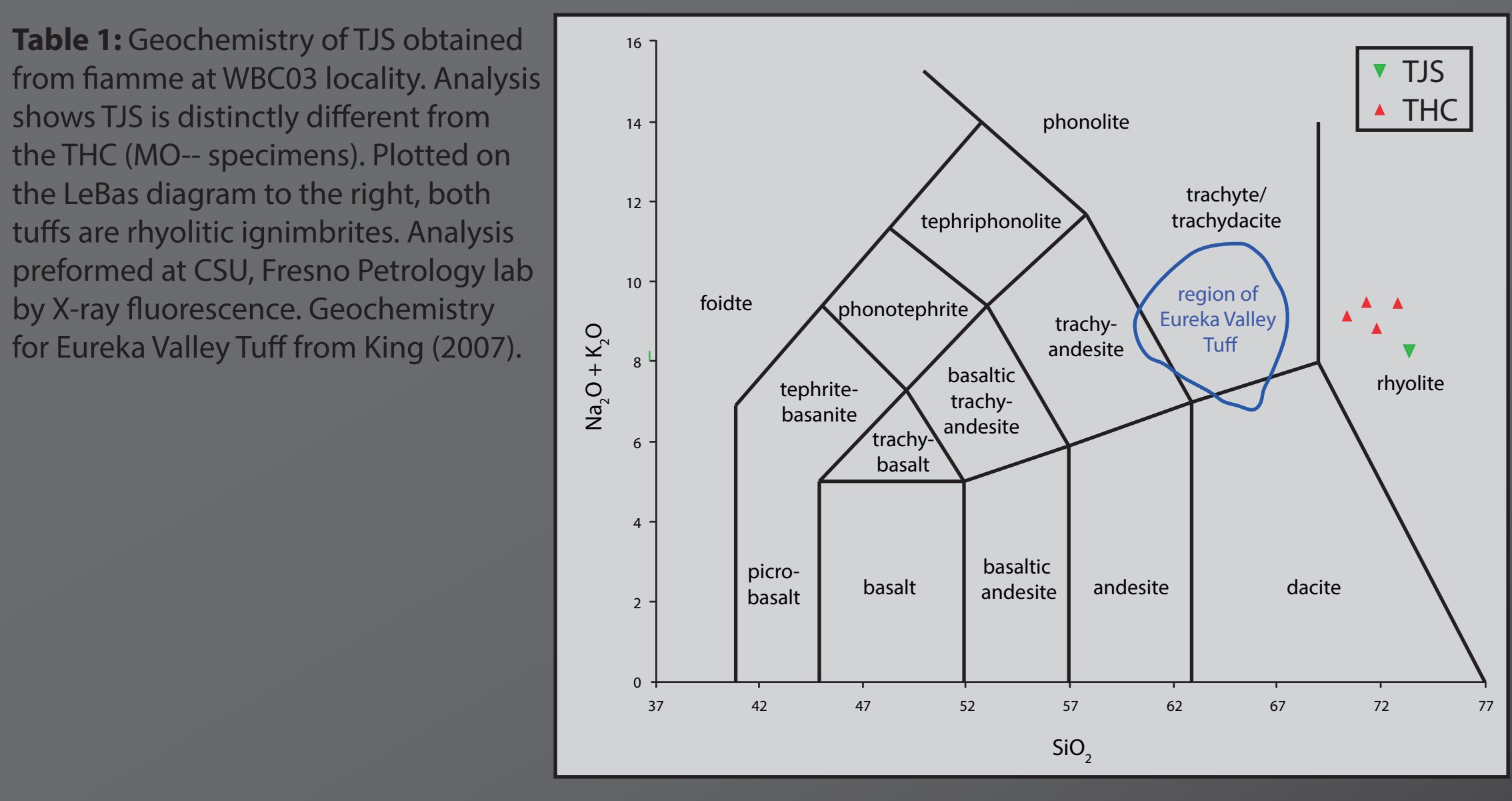


Figure 7: ChRM of MO01 without tilt corrected. Figure 8: ChRM of MO01 with tilt corrections. Figure 9: ChRM of HUN01 without tilt corrections. Figure 10: ChRM of HUN01 with tilt corrections. Figure 11: ChRM of HUN02 without tilt corrections. Figure 12: ChRM of HUN02 with tilt corrections. Figures 9–12 demagnetized at Caltech Paleomagnetism Laboratory from NRM to 90 mT. Red star indicates Fisher mean. Figure 13: ChRM of FNR01 without tilt corrections. Figure 14: ChRM of FNR01 with tilt corrections. The outliers, indicated by blue in Figures 13 and 14, were lightning struck and loose before orientation (LBO), respectively, and were not included in the Fisher mean statistics.

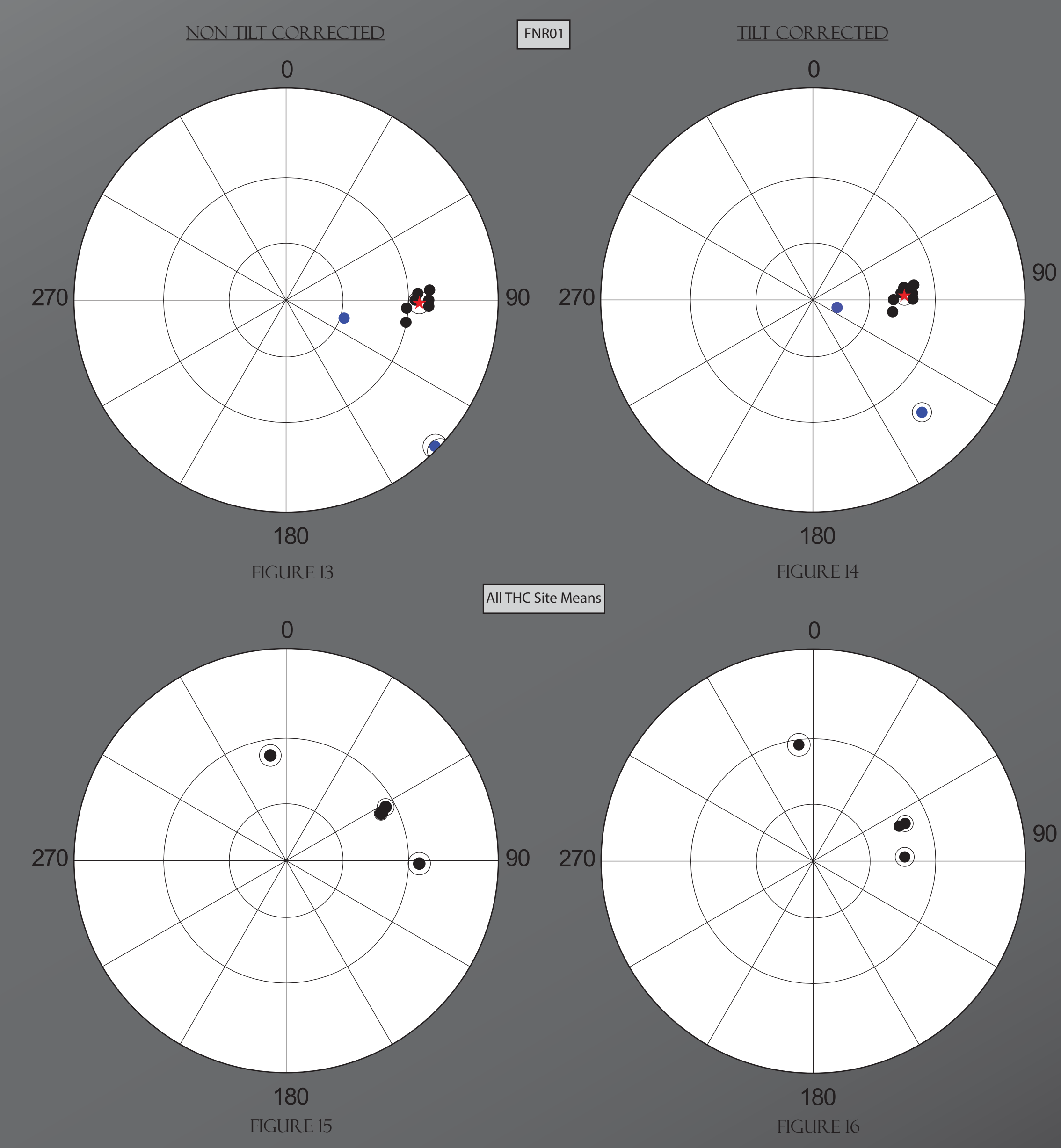


Figure 13: Means of THC ChRMs without tilt corrections. Figure 14: Means of THC ChRMs with tilt corrections.

Special thanks: AGICO JR6, Brandy Anglen, Sue Bratcher, Fresno Gem and Mineral Society, Shelby Fredrickson, Tommy Fredrickson, Jonathan Glen, David John, Shelby Jones, Bob Lindeman, Debbie Lindeman, Kevin Loeb, Scott Mitchell, Craig Poole, Keith Putirka, Belinda Rossette, Melissa Scruggs, Kelly Townsend, Brent Vanderburgh, John Wakabayashi

Locality	Declination (D)	Inclination (I)	Rotation	Flattening	Alpha 95	Declination (D)	Inclination (I)	Rotation	Flattening
MO01	351.4°	36.8°			4.7°	352.9°	32.1°		
HUN01	63.6°	37.0°	-72.2° ± 5.5	-0.2° ± 4.4	2.9°	67.8°	42.8°	-74.9° ± 5.5	-10.7° ± 4.4
HUN02	61.7°	33.9°	-70.3° ± 5.8	2.9° ± 4.7	3.6°	67.7°	39.8°	-74.8° ± 5.8	-7.7° ± 4.4
FNR01	91.3°	25.9°	-99.9° ± 6.1	10.9° ± 5.1	4.3°	87.4°	43.3°	-94.5° ± 6.5	-11.2° ± 5.1
VCE01	357.8°	39.6°			4.4°	333.7°	34.9°		
VCE02	6.4°	50.0°	-8.6° ± 5.7	-10.4° ± 4.1	2.7°	354.4°	45.3°	-380.7° ± 5.3	-10.4° ± 4.1
WBC03	349.7°	37.2°	-351.9° ± 5.2	2.4° ± 4.0	2.4°	14.5°	50.0°	-40.8° ± 5.2	-15.1° ± 4.0
WBC04	349.1°	46.3°	-351.3° ± 5.2	-6.7° ± 3.9	2.1°	2.1°	41.5°	-28.4° ± 4.8	-6.6° ± 3.9
WBC05	346.5°	38.1°	-348.7° ± 9.7	-1.5° ± 7.6	8.4°	353.5°	33.7°	-379.8° ± 9.2	1.2° ± 7.6

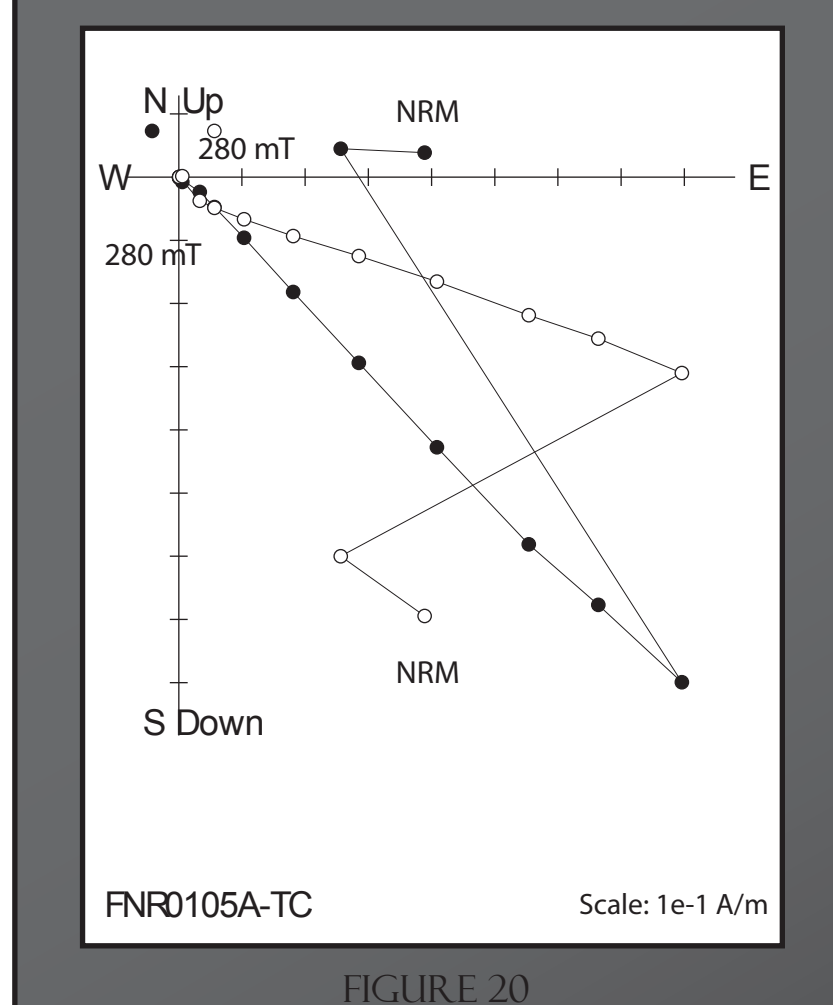
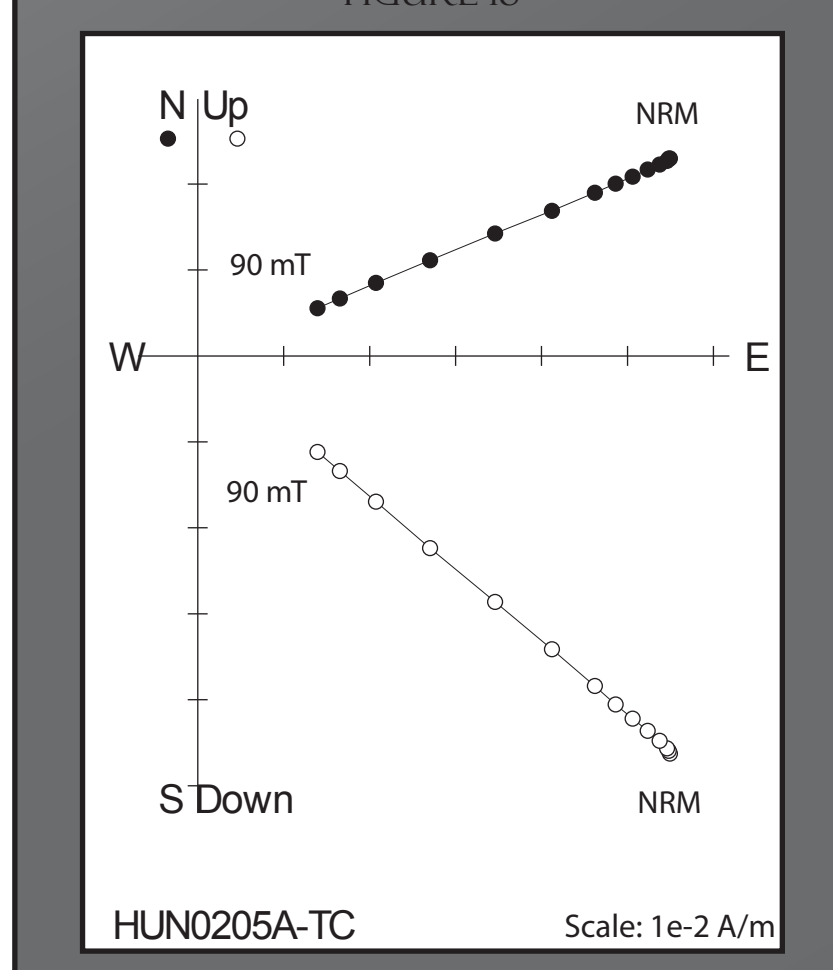
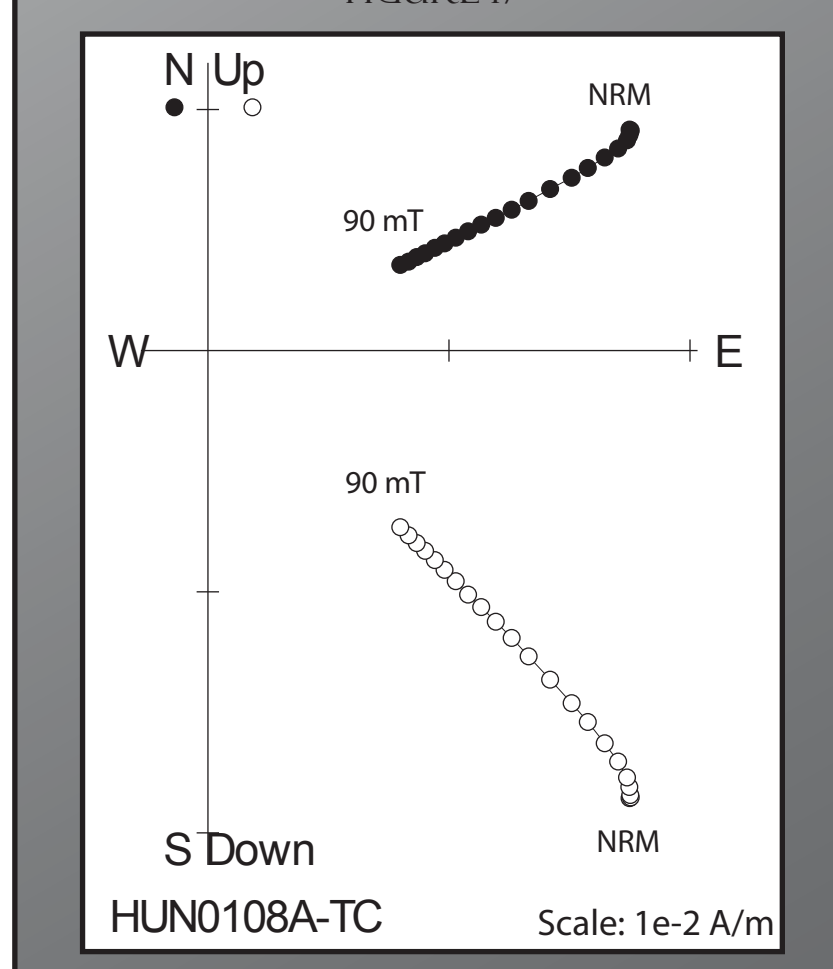
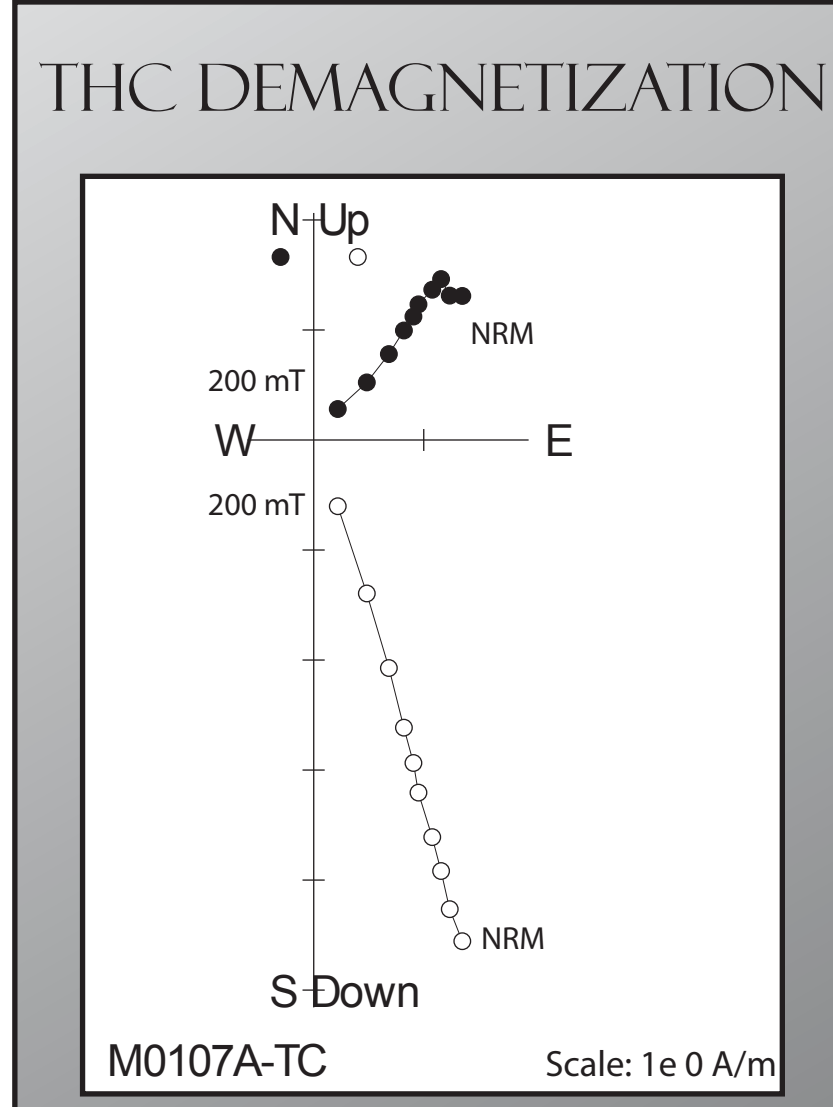


Figure 18–19: Demagnetized at Caltech Paleomagnetism Lab at NRM, 2, 4, 7, 10, 14, 18, 22, 26, 30, 35, 40, 45, 50, 55, 60, 65, 70, 75, 80, 85, and 90 mT.

Locality	Declination (D)	Inclination (I)	Rotation	Flattening	Alpha 95	Declination (D)	Inclination (I)	Rotation	Flattening
MO01	351.4°	36.8°			4.7°	352.9°	32.1°		
HUN01	63.6°	37.0°	-72.2° ± 5.5	-0.2° ± 4.4	2.9°	67.8°	42.8°	-74.9° ± 5.5	-10.7° ± 4.4
HUN02	61.7°	33.9°	-70.3° ± 5.8	2.9° ± 4.7	3.6°	67.7°	39.8°	-74.8° ± 5.8	-7.7° ± 4.4
FNR01	91.3°	25.9°	-99.9° ± 6.1	10.9° ± 5.1	4.3°	87.4°	43.3°	-94.5° ± 6.5	-11.2° ± 5.1
VCE01	357.8°	39.6°			4.4°	333.7°	34.9°		
VCE02	6.4°	50.0°	-8.6° ± 5.7	-10.4° ± 4.1	2.7°	354.4°	45.3°	-380.7° ± 5.3	-10.4° ± 4.1
WBC03	349.7°	37.2°	-351.9° ± 5.2	2.4° ± 4.0	2.4°	14.5°	50.0°	-40.8° ± 5.2	-15.1° ± 4.0
WBC04	349.1°	46.3°	-351.3° ± 5.2	-6.7° ± 3.9	2.1°	2.1°	41.5°	-28.4° ± 4.8	-6.6° ± 3.9
WBC05	346.5°	38.1°	-348.7° ± 9.7	-1.5° ± 7.6	8.4°	353.5°	33.7°	-379.8° ± 9.2	1.2° ± 7.6

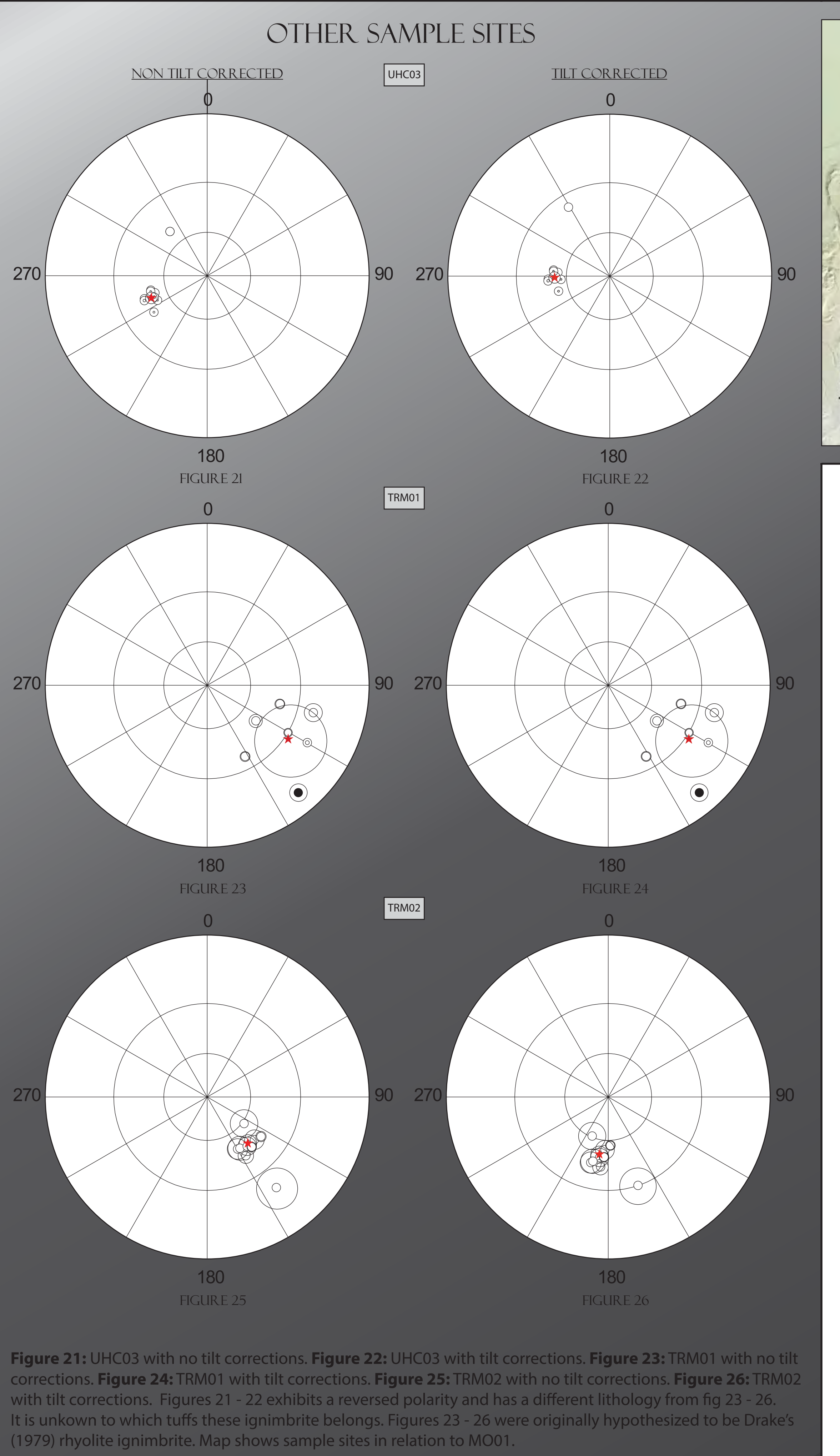


Figure 21: UHC03 with no tilt corrections. Figure 22: UHC03 with tilt corrections. Figure 23: TRM01 with no tilt corrections. Figure 24: TRM01 with tilt corrections. Figure 25: TRM02 with no tilt corrections. Figure 26: TRM02 with tilt corrections. Figures 21–22 exhibit a reversed polarity and has a different lithology from Figure 23–26. It is unknown to which tuffs these ignimbrites belong. Figures 23–26 were originally hypothesized to be Drake's (1979) rhyolite ignimbrite. Map shows sample sites in relation to MO01.

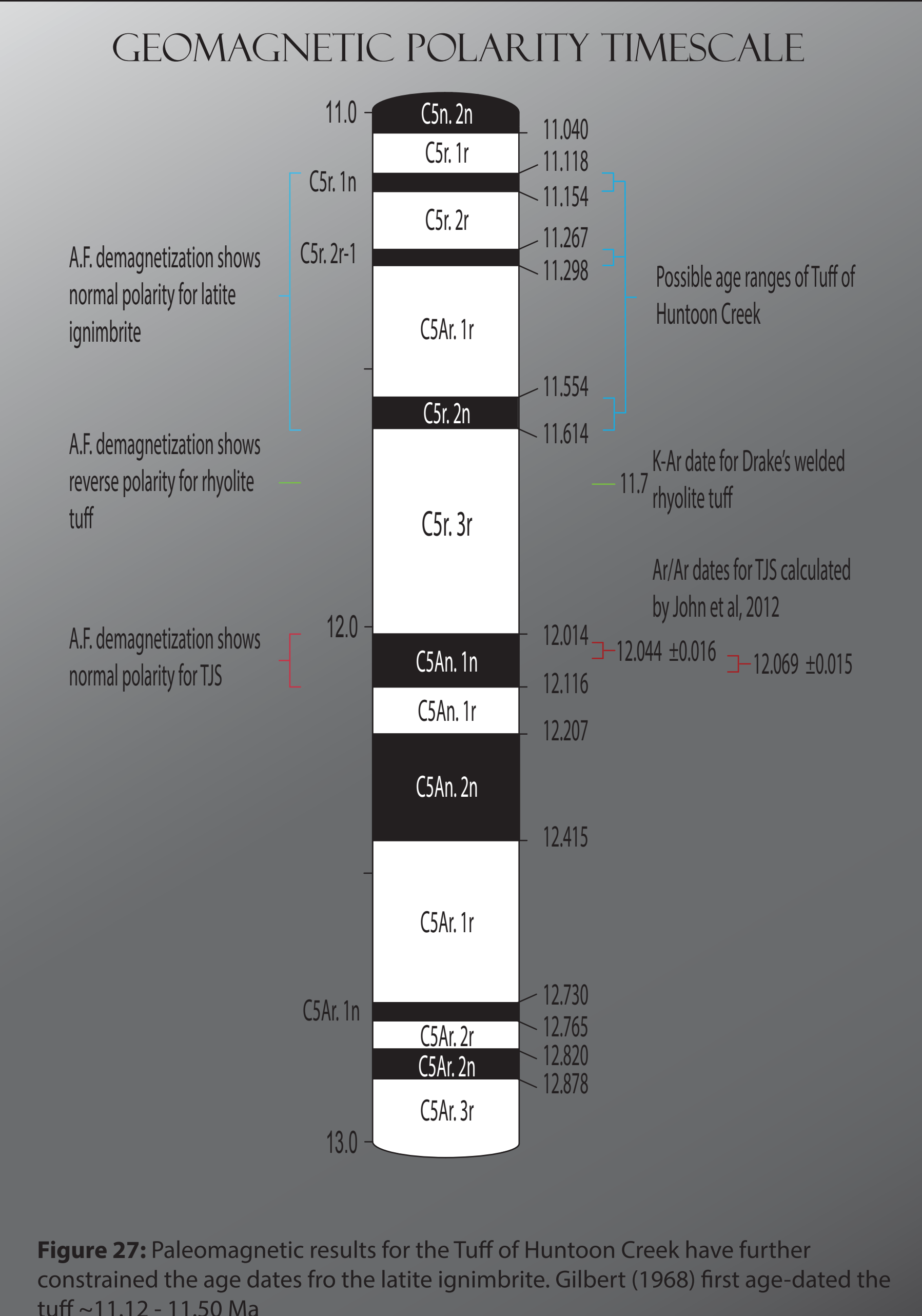
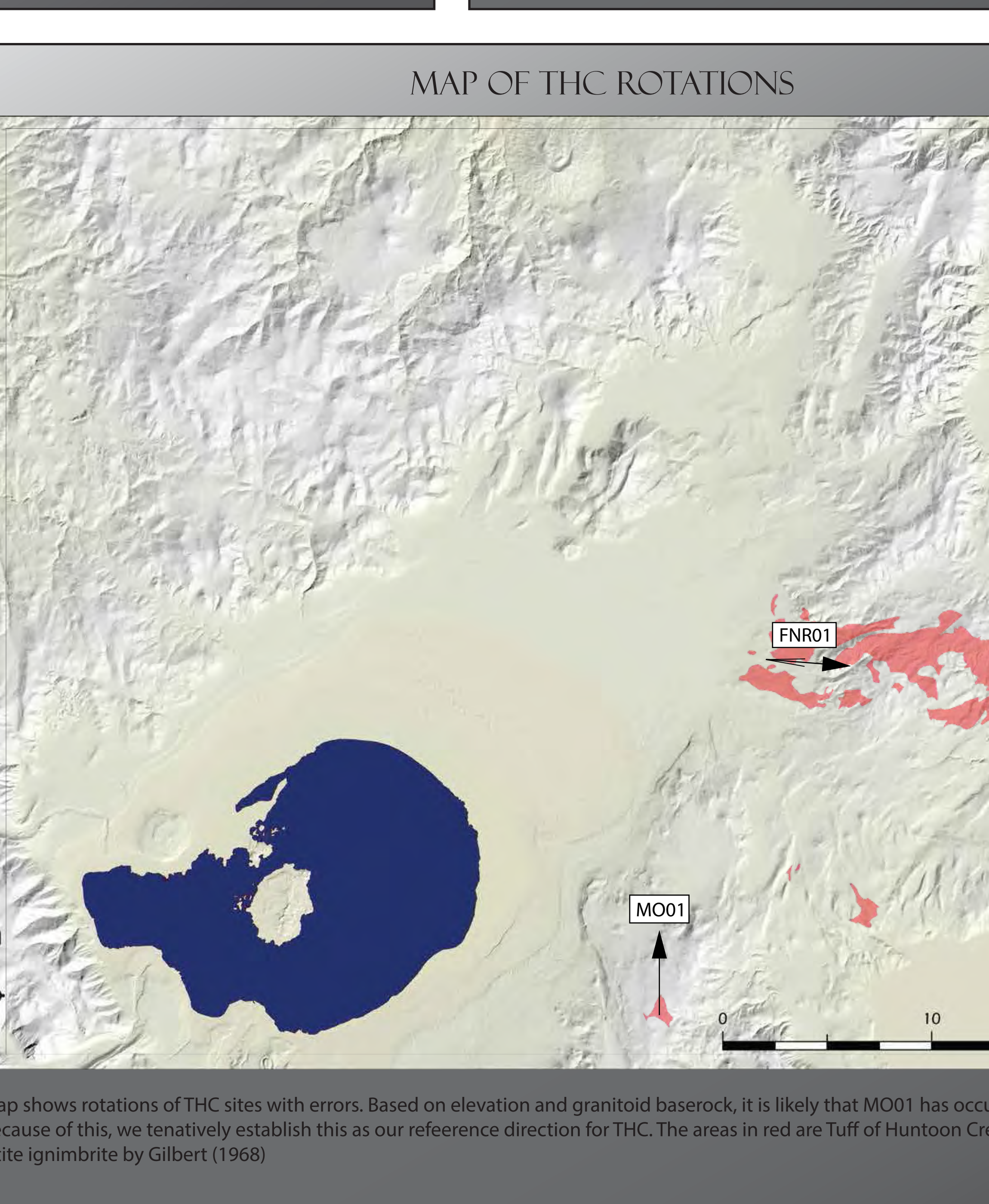
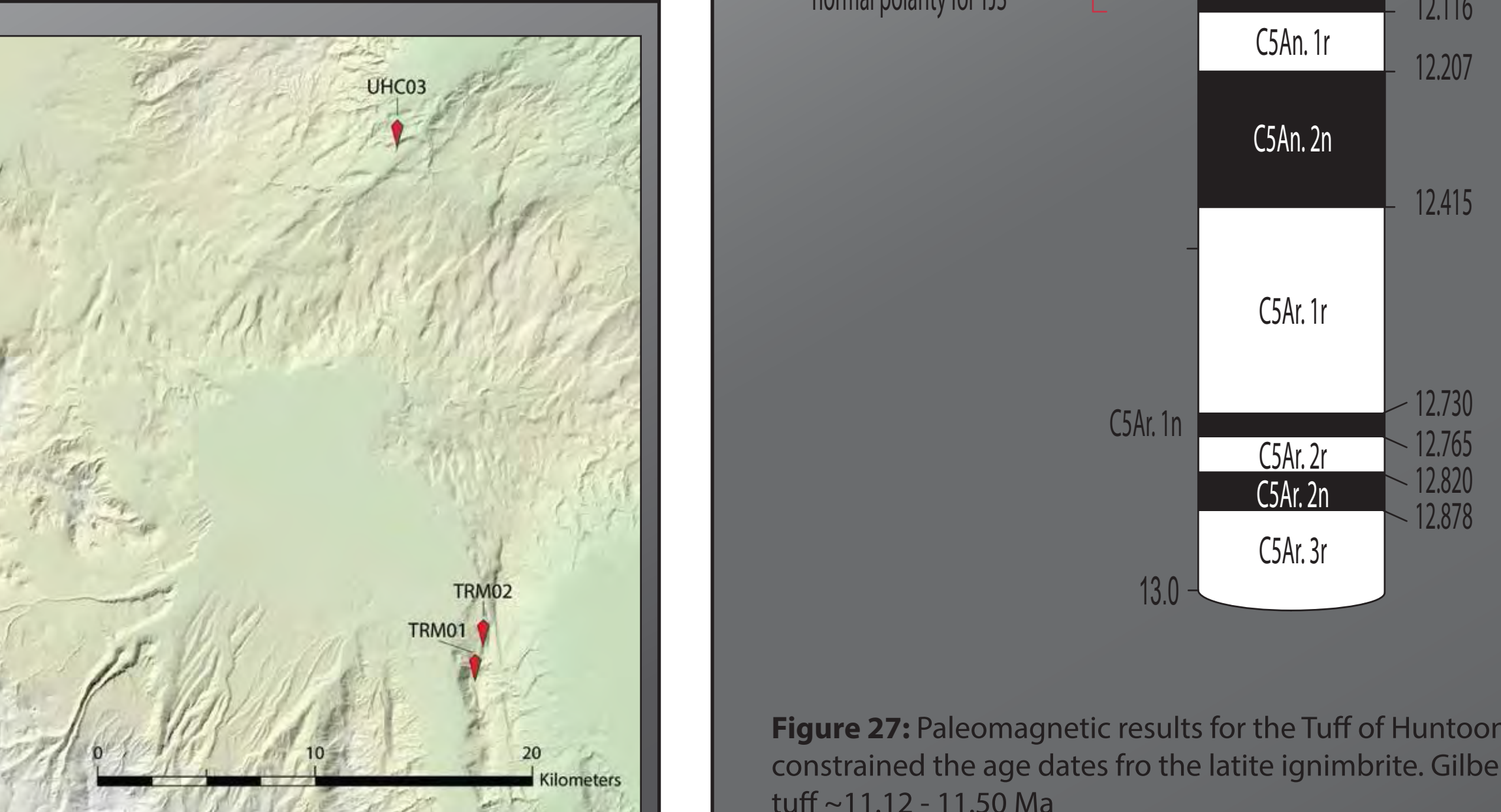


Figure 27: Paleomagnetic results for the Tuff of Hutton Creek have further constrained the age dates for the latite ignimbrite. Gilbert (1968) first age-dated the tuff ~11.12–11.50 Ma

References  
— Anderson, R.E., Berger, B.R., Higgins, D., 2012. Timing, magnitude, and style of Miocene deformation, west-central Walker Lane belt, Nevada. *Lithosphere*, v. 4, p. 187–208.  
— Carlson, C.W., 2012. Changes in Central Walker Lane accommodation near Bridgeport, California, as told by the Statistical Group. (M.S. thesis): California State University, Fresno.  
— Gilbert, C.M., Christiansen, N.M., Al-Rawi, Y., and Lajoie, K.R., 1968. Structural and volcanic history of Mono Basin, California-Nevada. *Mem. Geol. Soc. Am.*, v. 116, p. 275–325.  
— King, N.W., Hillhouse, W., Gromme, S., Haselback, B.P., and Fluhar, C.J., 2007. Stratigraphy, paleomagnetism, and anisotropy. *Geosphere*, v. 3, no. 6, p. 646–666.  
— Kleinhampl, G.J., Davis, W.E., Silberman, M.L., Chestman, C.H., Chapman, R.H., 1975. Aeromagnetic and Limited Gravity Studies and Generalized. *USGS Bulletin* 1384.  
— Oldow, J.S., Gessman, J.W., and Stockli, D.F., 2008. Evolution and Strain Reorganization within LateNeogene Structural Stoppers Linking the Central Walker Lane. *International Geology Review*, 50, 3, 270–290.  
— Stewart, J.H., Kleinhampl, G.J., Speed, R.C., Johannesen, D.C., 1984. Geologic map of the Little Hutton Valley quadrangle, Mineral County, Nevada.  
— Urrut, J., Humphrey, J., Barron, A., 2003. Transversal Model for the Sierra Nevada Frontal Fault System, Eastern California. *Geology*, v. 31, p. 327–330.